Week 11
Lecture Notes:
Topological Condensed Matter Physics

Sebastian Huber and Titus Neupert

Department of Physics, ETH Zürich
Department of Physics, University of Zürich

Chapter 11

Kitaev's Honeycomb Model and the Toric code

Learning goals

- We know the physical motivation, Hamiltonian, and phase diagram of Kitaev's honeycomb model.
- We understand how some phases reduce to the toric code Hamiltonian.
- We know how to rewrite the ground state and low-lying excitations in terms of Majorana degrees of freedom.
- We know the toric code model Hamiltonian and understand its ground state manifold.
- We know the emergent excitations above the ground states, and how to derive their statistics.

- A. Kitaev, Annals of Physics **321**, 2–111 (2006)

So far, we have been concerned with symmetry protected topological states and considered examples that were motivated by the topological classification of free fermion Hamiltonians. The topological properties of these systems are manifest by the presence of protected boundary modes. In this Chapter, we want to familiarize ourselves with the concept of intrinsic topological order by ways of several examples. We will study the connections between different characterizations of topological order, such as fractionalized excitations in the bulk and the topological ground state degeneracy. Our examples will be in 2D space, as topologically ordered states do not exist in 1D and are best understood in 2D.

11.1 Definition of the model

We want to physically motivate the following Hamiltonian

$$H = -J_x \sum_{x-\text{links}} \sigma_j^x \sigma_k^x - J_y \sum_{y-\text{links}} \sigma_j^y \sigma_k^y - J_z \sum_{z-\text{links}} \sigma_j^z \sigma_k^z, \tag{11.1.1}$$

acting on spin 1/2 degrees of freedom on a honeycomb lattice, where the bonds in the 3 inequivalent directions have been labeled x, y, z. This Hamiltonian has been proposed to be relevant to the honeycomb iridates Na_2IrO_3 and Li_2IrO_3, see Fig. 11.1, and there is mounting experimental evidence that α-$RuCl_3$ is governed (in part) by this Hamiltonian. In addition, there is a Heisenberg term allowed and competing with this term in the materials, but since we are interested in the physics in some integrable limit, we consider the Hamiltonian (11.1.1) on its own right.
A model is called integrable if it has an extensive number of integrals of motion. In what we studied so far, we have simply used the powers of the primitive translation operator (or the momentum operator) as the conserved quantities. For Hamiltonian (11.1.1), we can construct

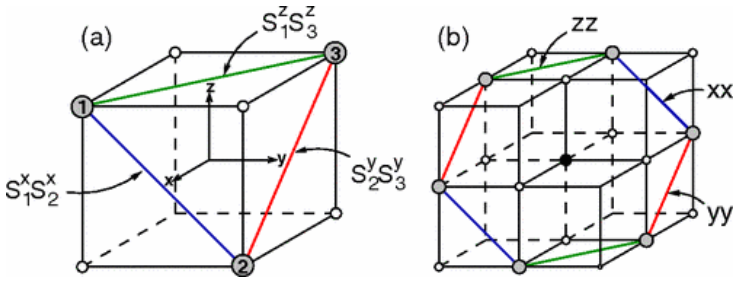

Figure 11.1: Examples of the structural units formed by 90 degree TM-O-TM bonds and corresponding spin-coupling patterns. Gray circles stand for magnetic ions (e.g., Ir), and small open circles denote oxygen sites, and black is sodium, for example. From [PRL **102**, 017205 (2009)]. Spins come from the Ir 5d orbitals, which in the octahedral coordination split in t_{2g} and e_g. The former further split into a $j = 1/2$ and a $j = 3/2$ sector by spin-orbit coupling. In the $j = 1/2$ sector, the 90 degree Ir-O-Ir bonds give rise to the Kitaev exchange interaction.

local conserved quantities as follows: consider around any plaquette p of the hexagonal lattice the operator

$$W_p = \sigma_1^x \sigma_2^y \sigma_3^z \sigma_4^x \sigma_5^y \sigma_6^z, \tag{11.1.2}$$

where $1 \cdots 6$ label the sites around the plaquette in such a way that the link leading out of the plaquette from site i is a $\alpha = x, y, z$ link if σ_i^α appears in W_p [see Fig. 11.2 a)]. Observe that W_p has eigenvalues ± 1 and commutes with the Hamiltonian. Thus the Hilbert space splits up in sectors with fixed eigenvalues $w_p = \pm 1$ of each operator W_p. The honeycomb lattice has $1/2$ plaquette per spin, hence for N vertices the total Hilbert space dimension 2^N is reduced to $2^{N/2}$ subspaces of dimension $2^{N/2}$. Hence, the problem is not completely solved by splitting it into w_p sectors, but we made some progress still.
Further progress can be made by representing the spins in terms of Majorana operators: Consider at every site j of the honeycomb lattice four Majorana operators b_j^x, b_j^y, b_j^z, and c_j, which obey the usual relations

$$\{b_j^\alpha, b_j^{\alpha'}\} = 2\delta_{\alpha,\alpha'}, \qquad \{b_j^\alpha, c_j\} = 0, \qquad c_j^2 = 1. \tag{11.1.3}$$

Four Majorana operators furnish a 4-dimensional Hilbert space $\tilde{\mathcal{M}}_j$ (one can build 2 complex fermions from them). This is twice as large as the Hilbert space of a single spin. We reduce $\tilde{\mathcal{M}}_j$ to a physical subspace $\mathcal{M}_j \subset \tilde{\mathcal{M}}_j$ by the following constraint

$$|\xi_j\rangle \in \mathcal{M}_j \qquad \Leftrightarrow \qquad D_j |\xi_j\rangle = |\xi_j\rangle, \tag{11.1.4}$$

where $D_j = b_j^x b_j^y b_j^z c_j$. We see that D_j is the total parity of the two fermionic levels defined from the four Majoranas. We now want to represent the Pauli operators on $\tilde{\mathcal{M}}_j$ such that the respective operators obey the same algebra on $\mathcal{M}_j$ and commute with D_j (i.e., they preserve the subspace $\mathcal{M}_j$). We choose

$$\tilde{\sigma}_j^\alpha = \mathrm{i} b_j^\alpha c_j, \qquad \alpha = x, y, z. \tag{11.1.5}$$

Observe that $\tilde{\sigma}_j^x \tilde{\sigma}_j^y \tilde{\sigma}_j^z = \mathrm{i} D_j$, and D_j is the identity on $\mathcal{M}_j$, compatible with $\sigma_j^x \sigma_j^y \sigma_j^z = \mathrm{i}$.
We can use this Majorana representation to rewrite all the terms in our Hamiltonian

$$\sigma_j^\alpha \sigma_k^\alpha \to (\mathrm{i} b_j^\alpha c_j)(\mathrm{i} b_k^\alpha c_k) = -\mathrm{i}(\mathrm{i} b_j^\alpha b_k^\alpha) c_j c_k, \tag{11.1.6}$$

where $\alpha = x, y, z$ is not summed over. We can rewrite

$$\tilde{H} = \frac{\mathrm{i}}{4} \sum_{j,k} \hat{A}_{jk} c_j c_k \tag{11.1.7}$$

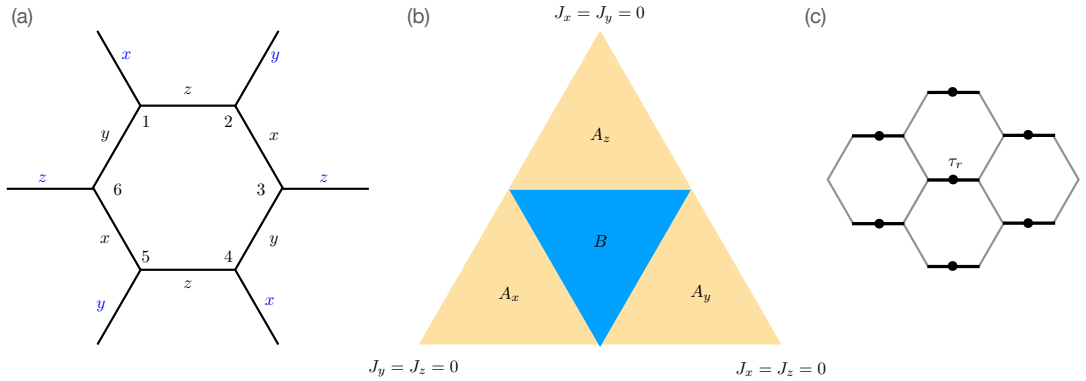

Figure 11.2: a) Definition of x, y, z type bonds for the Kitaev Hamiltonian (11.1.1) on the honeycomb lattice and of the numbering of sites within a plaquette that enter the W_p operator (11.1.2). b) Phase diagram of the Kitaev honeycomb model. c) Strong bonds that are replaced with an effective spin-1/2 degree of freedom in the limit $|J_z| \gg |J_x|, |J_y|$ to derive the toric code Hamiltonian.

where $\hat{A}_{jk} = 2J_{\alpha_{jk}} \hat{u}_{ik}$ is a hermitian operator when i and j are connected and 0 otherwise. We defined $\hat{u}_{jk} := \mathrm{i} b_j^\alpha b_k^\alpha$ which commutes with the Hamiltonian and with the other $\hat{u}_{j'k'}$. Each $\hat{u}_{jk}$ has eigenvalues $u_{jk} = \pm 1$ and in each sector we can simply obtain the Hamiltonian by replacing operators by numbers, i.e.,$\hat{A}_{jk} \to A_{jk} = 2J_{\alpha_{jk}} u_{ik}$. However, observe that $\{\hat{u}_{jk}, D_j\} = 0$, i.e., $\hat{u}_{jk}$ does not leave the subspace $\mathcal{M}_j$ invariant. Starting from a ground state $|\tilde{\Psi}_u\rangle$ of $\tilde{H}_u = \frac{\mathrm{i}}{4} \sum_{j,k} A_{jk} c_j c_k$, we can construct a state

$$|\Psi_w\rangle = \prod_j \left(\frac{1 + D_j}{2} \right) |\tilde{\Psi}_u\rangle, \tag{11.1.8}$$

where w is the collection of eigenvalues w_p for each plaquette operator W_p. In therms of the Majorana bilinear eigenvalues they are given by $w_p = \prod_{j,k \in \partial p; j<k} u_{jk}$.
The lowest energy state is obtained if all $u_{jk} = +1$, which is a nontrivial statement. The relevant Hamiltonian is given by

$$H_{\text{vortex-free}} = \frac{\mathrm{i}}{4} \sum_{\boldsymbol{k}} \begin{pmatrix} c_{-\boldsymbol{k},A} & c_{-\boldsymbol{k},B} \end{pmatrix} \begin{pmatrix} 0 & \mathrm{i} f(\boldsymbol{k}) \\ -\mathrm{i} f(\boldsymbol{k})^* & 0 \end{pmatrix} \begin{pmatrix} c_{\boldsymbol{k},A} \\ c_{\boldsymbol{k},B} \end{pmatrix} \tag{11.1.9}$$

where

$$f(\boldsymbol{k}) = 2(J_x e^{\mathrm{i}\boldsymbol{k}\cdot\boldsymbol{a}_1} + J_y e^{\mathrm{i}\boldsymbol{k}\cdot\boldsymbol{a}_2} + J_z), \qquad \boldsymbol{a}_1 = \frac{1}{2}(1, \sqrt{3}), \quad \boldsymbol{a}_2 = \frac{1}{2}(-1, \sqrt{3}). \tag{11.1.10}$$

The spectrum corresponds to that of anisotropic graphene. Time-reversal symmetry and inversion symmetry, which protect the Dirac cones, are retained. Hence the system can only gap out if the anisotropy is large enough for two cones to meet (at one of the TRIM points). Said differently, zero energy solutions $J_x e^{\mathrm{i}\boldsymbol{k}\cdot\boldsymbol{a}_1} + J_y e^{\mathrm{i}\boldsymbol{k}\cdot\boldsymbol{a}_2} + J_z = 0$ are obtained if and only if

$$|J_x| \leq |J_y| + |J_z|, \qquad |J_y| \leq |J_x| + |J_z|, \qquad |J_z| \leq |J_x| + |J_y|. \tag{11.1.11}$$

This gives a phase diagram with three gapped phases A_x, A_y, A_z and a gapless phase B [see Fig. 11.2 b)]. The gapless phase has Majorana Dirac cones.

11.2 The gapped phases

Topological properties of a gapped phase are constant throughout the phase and we may study them in a parameter regime that is convenient for us. We will focus on the phase A_z and study it in the limit $|J_z| \gg |J_x|, |J_y|$. The Hamiltonian is given by $H = H_0 + V$ where

$$H_0 = -J_z \sum_{z-\text{links}} \sigma_j^z \sigma_k^z, \qquad V = -J_x \sum_{x-\text{links}} \sigma_j^x \sigma_k^x - J_y \sum_{y-\text{links}} \sigma_j^y \sigma_k^y, \tag{11.2.1}$$

is the dominant term and the perturbation, respectively. Out of two spins connected by a z-link, H_0 selects the states where these spins are both parallel or anti-parallel [see Fig. 11.2 c)]. We may thus replace these two spins by a single spin 1/2, which is acted upon with the V perturbation. Let us act on these spins with Pauli matrices τ_r^α to distinguish them from the original spins. The sites r live now on the links of a square lattice. It turns out that, to get back to the degenerate ground state subspace of H_0, one needs to apply the perturbation V 4 times. After going to fourth order in perturbation theory, and applying a unitary transformation, we obtain the Hamiltonian

$$H_{\text{eff}} = -J_{\text{eff}} \left(\sum_s A_s + \sum_p B_p \right) \tag{11.2.2}$$

where $J_{\text{eff}} = J_x^2 J_y^2 / (16|J_z|^3)$. Here, the four spins that sit on the bonds emanating from a given site r of the lattice are referred to as a star s. The four spins that sit on the bonds surrounding a square of the lattice are called a plaquette p. We defined two sets of operators

$$A_s := \prod_{r \in s} \tau_r^x, \qquad B_p := \prod_{r \in p} \tau_r^z. \tag{11.2.3}$$

We will analyze this exact same Hamiltonian in the following section.

11.3 Gapping the gapless phase

The gapless phase B has both vortex-like excitations which are gapped and fermionic excitations which are gapless (they live on a Majorana cone). The statistics of the vortices is not well defined due to the interaction with the gapless fermionic background. The gapless nature of the fermions is protected by (inversion times) time-reversal symmetry, just as in graphene. This is true for all flux sectors, as $\mathbb{Z}_2$ flux does not break time-reversal symmetry. The fermions can, however, be gapped out when breaking time-reversal symmetry. Consider applying an external magnetic field

$$\delta H_{\text{B}} = -\sum_j \boldsymbol{B} \cdot \boldsymbol{\sigma}_j. \tag{11.3.1}$$

Kitaev showed that in the vortex-free sector, the time-reversal symmetry breaking nature of this term manifests to third order in perturbation theory (for $J_x = J_y = J_z = J$) as

$$\delta H_{\text{B}}^{(3)} = -\frac{B_x B_y B_z}{J^2} \sum_{i,k,l} \sigma_j^x \sigma_k^y \sigma_l^z, \tag{11.3.2}$$

where sites j, k, l are clockwise neighbors belonging to s single hexagon (i.e., there are six such terms in each hexagon). In the fermionic language

$$\begin{aligned} \sigma_j^x \sigma_k^y \sigma_l^z =& (\mathrm{i} b_j^x c_j)(\mathrm{i} b_k^y c_k)(\mathrm{i} b_l^z c_l) \\ =& -\mathrm{i} b_j^x c_j \, b_k^x b_k^x \, b_k^y c_k \, b_k^z b_k^z \, b_l^z c_l \\ =& -\mathrm{i} (b_k^x b_k^y b_k^z c_k)(b_j^x b_k^x)(b_k^z b_l^z) c_j c_l \\ =& +\mathrm{i} D_k \hat{u}_{jk} \hat{u}_{kl} c_j c_l. \end{aligned} \tag{11.3.3}$$

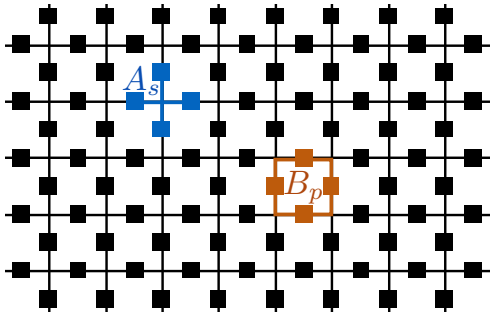

Figure 11.3: The toric code model is defined on a square lattice with spin-1/2 degrees of freedom on every bond (black squares). The operator A_s acts with σ_x on all four spins one the bonds that are connected to a lattice site (a star s). The operator B_p acts with σ_z on all four spins around a plaquette p.

Omitting D in the physical subspace and using the standard gauge, $\hat{u}_{jk} = \hat{u}_{kl} = 1$, we have a term $\mathrm{i}c_j c_l$ which is exactly the NNN hopping of the Haldane model with $\phi = \pi/2$ and $t_2 \sim B_x B_y B_z / J^2$. Thus, with the magnetic field switched on, the Majorana fermion bands acquire a Chern number ± 1. We thus have a model formally equivalent to the chiral p-wave superconductor, with the important difference that the $\mathbb{Z}_2$ vortices are *dynamic* objects this time, i.e., the system is properly topologically ordered with non-Abelian Majorana anyons σ (a vortex) and the same properties as discussed before.

11.4 The toric code

As an example of a topologically ordered state we study an exactly soluble model with vanishing correlation length. The significance of having zero correlation length is the following. The correlation functions of local operators decay exponentially in gapped quantum ground states in 1D and 2D with a characteristic length scale given by the correlation length ξ. In contrast, topological properties are encoded in quantized expectation values of nonlocal operators (for example the Hall conductivity) or the degeneracy of energy levels (such as the end states of the Su-Schrieffer-Heeger model). In finite systems, such quantizations and degeneracies are generically only exact up to corrections that are of order $e^{-L/\xi}$, where L is the linear system size. Models with zero correlation length are free from such exponential finite-size corrections and thus expose the topological features already for the smallest possible system sizes. The down-side is that their Hamiltonians are rather contrived.
We define the toric code model on a square lattice with a spin-1/2 degree of freedom on every *bond* j (see Fig. 11.3). The four spins that sit on the bonds emanating from a given site of the lattice are referred to as a star s. The four spins that sit on the bonds surrounding a square of the lattice are called a plaquette p. We define two sets of operators

$$A_s := \prod_{j \in s} \sigma_j^x, \qquad B_p := \prod_{j \in p} \sigma_j^z, \tag{11.4.1}$$

that act on the spins of a given star s and plaquette p, respectively. Here, $\sigma_j^{x,z}$ are the respective Pauli matrices acting on the spin on bond j.
These operators have two crucial properties which are often used to construct exactly soluble models for topological states of matter

1. All of the A_s and B_p commute with each other. This is trivial for all cases except for the commutator of A_s with B_p if s and p have spins in common. However, any star shares with

any plaquette an even number of spins (edges), so that commuting A_s with B_p involves commuting an even number of σ^z with σ^x, each of which comes with a minus sign.

2. The operators
$$\frac{1-B_p}{2}, \qquad \frac{1-A_s}{2} \tag{11.4.2}$$
are projectors. The former projects out plaquette states with an even number of spins polarized in the positive z-direction. The latter projects out stars with an even number of spins in the positive x-direction.

11.4.1 Ground states

The Hamiltonian is defined as a sum over these commuting projectors

$$H = -J_{\mathrm{e}} \sum_s A_s - J_{\mathrm{m}} \sum_p B_p, \tag{11.4.3}$$

where the sums run over all stars s and plaquettes p of the lattice. Let us assume that both J_{e} and J_{m} are positive constants. Then, the ground state is given by a state in which all stars s and plaquettes p are in an eigenstate with eigenvalue $+1$ of A_s and B_p, respectively. (The fact that all A_s and B_p commute allows for such a state to exist, as we can diagonalize each of them separately.) Let us think about the ground state in the eigenbasis of the σ^x operators and represent by bold lines those bonds with spin up and and draw no lines along bonds with spin down. Then, A_s imposes on all spin configurations with nonzero amplitude in the ground state the constraint that an even number of bold lines meets at the star s. In other words, we can think of the bold lines as connected across the lattice and they may only form closed loops. Bold lines that end at some star ("open strings") are not allowed in the ground state configurations; they are excited states. Having found out which spin configurations are allowed in the ground state, we need to determine their amplitudes. This can be inferred from the action of the B_p operators on these closed loop configurations. The B_p flips all bonds around the plaquette p. Since $B_p^2 = 1$, given a spin configuration $|c\rangle$ in the σ^x-basis, we can write an eigenstate of B_p with eigenvalue 1 as

$$\frac{1}{\sqrt{2}} \left(|c\rangle + B_p |c\rangle \right), \tag{11.4.4}$$

for some fixed p. This reasoning can be extended to all plaquettes so that we can write for the ground state

$$|\mathrm{GS}\rangle = \left(\prod_p \frac{1+B_p}{\sqrt{2}} \right) |c\rangle, \tag{11.4.5}$$

where $|c\rangle$ is a closed loop configuration [see Fig. 11.4 a)]. Is $|\mathrm{GS}\rangle$ independent of the choice of $|c\rangle$? In other words, in the ground state unique? We will see that the answer depends on the topological properties of the manifold on which the lattice is defined and thus reveals the topological order imprinted in $|\mathrm{GS}\rangle$.

To answer these questions, let us consider the system on two topologically distinct manifolds, the torus and the sphere. To obtain a torus, we consider a square lattice with $L_x \times L_y$ sites and impose periodic boundary conditions. This lattice hosts $2L_xL_y$ spins (2 per unit cell for they are centered along the bonds). Thus, the Hilbert space of the model has dimension $2^{2L_xL_y}$. There are L_xL_y operators A_s and just as many B_p. Hence, together they impose $2L_xL_y$ constraints on the ground state in this Hilbert space. However, not all of these constraints are independent. The relations

$$1 = \prod_s A_s, \qquad 1 = \prod_p B_p \tag{11.4.6}$$

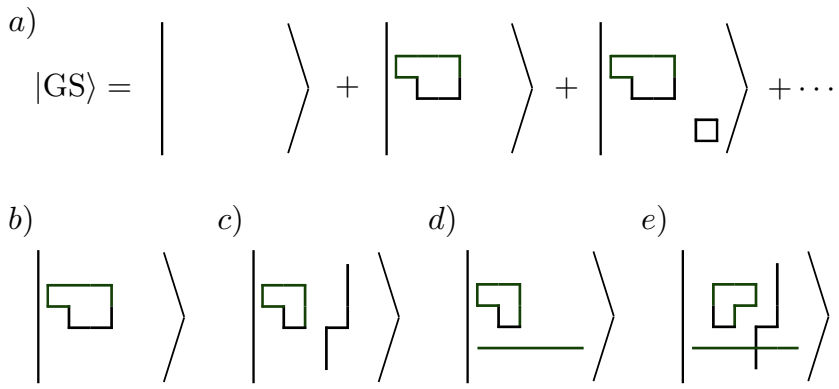

Figure 11.4: Visualization of the toric code ground states on the torus. a) The toric code ground state is the equal amplitude superposition of all closed loop configurations. b)-e) Four base configurations $|c\rangle$ entering Eq. (11.4.5) that yield topologically distinct ground states on the torus.

make two of the constraints redundant, yielding $(2L_xL_y - 2)$ independent constraints. The ground state degeneracy (GSD) is obtained as the quotient of the Hilbert space dimension and the subspace modded out by the constraints

$$\text{GSD} = \frac{2^{2L_xL_y}}{2^{2L_xL_y-2}} = 4. \tag{11.4.7}$$

The four ground states on the torus are distinguished by having an even or an odd number of loops wrapping the torus in the x and y direction, respectively. Four configurations $|c\rangle$ that can be used to build the four degenerate ground states are shown in Fig. 11.4 b)-e). This constitutes a set of "topologically degenerate" ground states and is a hallmark of the topological order in the model.

Let us contrast this with the ground state degeneracy on the sphere. Since we use a zero correlation length model, we might as well use the smallest convenient lattice with the topology of a sphere. We consider the model (11.4.3) defined on the edges of a cube. The same counting as above yields that there are 12 degrees of freedom (the spins on the 12 edges), 8 constraints from the A_s operators defined on the corners and 6 constraints from the B_p operators defined on the faces. Subtracting the 2 redundant constraints (11.4.6) yields $12-(8+6-2) = 0$ remaining degrees of freedom. Hence, the model has a unique ground state on the sphere.

On a general manifold, we have

$$\text{GSD} = 2^{\text{number of noncontractible loops}}. \tag{11.4.8}$$

An important property of the topologically degenerate ground states is that any local operator has vanishing off-diagonal matrix elements between them in the thermodynamic limit. Similarly, no local operator can be used to distinguish between the ground states. We can, however, define *nonlocal* operators that transform one topologically degenerate ground state into another and that distinguish the ground states by topological quantum numbers. (Notice that such operators may not appear in any physical Hamiltonian due to their nonlocality and hence the degeneracy of the ground states is protected.) On the torus, we define two pairs of so-called Wilson loop operators as

$$W^{\text{e}}_{x/y} := \prod_{j\in l^{\text{e}}_{x/y}} \sigma^z_j, \qquad W^{\text{m}}_{x/y} := \prod_{j\in l^{\text{m}}_{x/y}} \sigma^x_j. \tag{11.4.9}$$

Here, $l^{\text{e}}_{x/y}$ are the sets of spins on bonds parallel to a straight line wrapping the torus once along the x- and y-direction, respectively. The $l^{\text{m}}_{x/y}$ are the sets of spins on bonds perpendicular to a

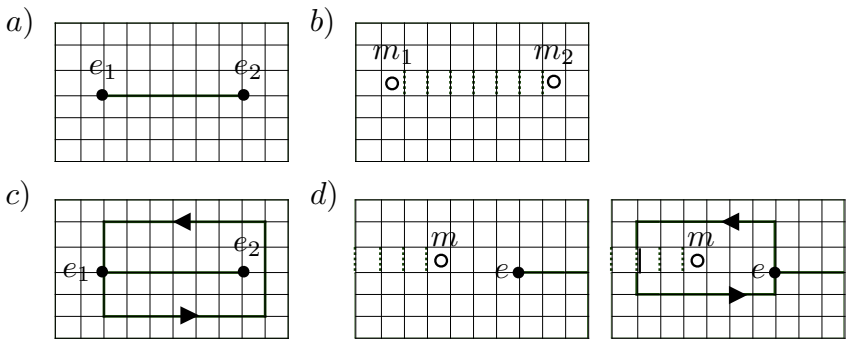

Figure 11.5: Visualization of operations to compute the braiding statistics of toric code anyons. a) Two e excitations above the ground state. b) Two m excitations above the ground state. c) Loop created by braiding e_1 around e_2. c) Loop created by braiding e around m. A phase of -1 results for this process because there is a single bond on which both a σ^x operator (dotted line) and a σ^z operator (bold line) act.

straight line that connects the centers of plaquettes and wraps the torus once along the x and y-direction, respectively. We note that the $W^{\mathrm{e}}_{x/y}$ and $W^{\mathrm{m}}_{x/y}$ commute with all A_s and B_p

$$\left[W^{\mathrm{e/m}}_{x/y}, A_s\right] = \left[W^{\mathrm{e/m}}_{x/y}, B_p\right] = 0, \tag{11.4.10}$$

and thus also with the Hamiltonian. Furthermore, they obey

$$W^{\mathrm{e}}_x W^{\mathrm{m}}_y = -W^{\mathrm{m}}_y W^{\mathrm{e}}_x. \tag{11.4.11}$$

This algebra must be realized in any eigenspace of the Hamiltonian. However, due to Eq. (11.4.11), it cannot be realized in a one-dimensional subspace. We conclude that all eigenspaces of the Hamiltonian, including the ground state, must be degenerate. In the σ^x basis that we used above, $W^{\mathrm{m}}_{x/y}$ measures whether the number of loops wrapping the torus is even or odd in the x and y direction, respectively, giving 4 degenerate ground states. In contrast, $W^{\mathrm{e}}_{x/y}$ changes the number of loops wrapping the torus in the x and y direction between even and odd.

11.4.2 Topological excitations

To find the topological excitations of the system above the ground state, we ask which are the lowest energy excitations that we can build. Excitations are a violation of the rule that all stars s are eigenstates of A_s and all plaquettes p are eigenstates of B_p. Let us first focus on star excitations which we will call e. They appear as the end point of open strings, i.e., if the closed loop condition is violated. Since any string has two end points, the lowest excitation of this type is a pair of e. They can be created by acting on the ground state with the operator

$$W^{\mathrm{e}}_{l^{\mathrm{e}}} := \prod_{j \in l^{\mathrm{e}}} \sigma^z_j, \tag{11.4.12}$$

where l^{e} is a string of bonds connecting the two excitations e_1 and e_2 [see Fig. 11.5 a)]. The state

$$|e_1, e_2\rangle := W^{\mathrm{e}}_{l^{\mathrm{e}}}|\mathrm{GS}\rangle \tag{11.4.13}$$

has energy $4J_{\mathrm{e}}$ above the ground state energy. Similarly, we can define an operator

$$W^{\mathrm{m}}_{l^{\mathrm{m}}} := \prod_{j \in l^{\mathrm{m}}} \sigma^x_j, \tag{11.4.14}$$

that creates a pair of plaquette defects m_1 and m_2 connected by the string l^{m} of perpendicular bonds [see Fig. 11.5 b)]. (Notice that the operator $W^{\mathrm{m}}_{l^{\mathrm{m}}}$ does not flip spins when the ground state is written in the σ^x basis. Rather, it gives weight $+1/-1$ to the different loop configurations in the ground state, depending on whether an even or an odd number of loops crosses l^{m}.) The state

$$|m_1, m_2\rangle := W^{\mathrm{m}}_{l^{\mathrm{m}}}|\mathrm{GS}\rangle \tag{11.4.15}$$

has energy $4J_{\mathrm{m}}$ above the ground state energy. Notice that the excited states $|e_1, e_2\rangle$ and $|m_1, m_2\rangle$ only depend on the positions of the excitations and not on the particular choice of string that connects them. Furthermore, the energy of the excited state is independent of the separation between the excitations. The excitations are thus "deconfined", i.e., free to move independent of each other.

It is also possible to create a combined defect when a plaquette hosts a m excitation and one of its corners hosts a e excitation. We call this combined defect f and formalize the relation between these defects in a so-called fusion rule

$$e \times m = f. \tag{11.4.16a}$$

When two e-type excitations are moved to the same star, the loop l^{e} that connects them becomes a closed loop and the state returns to the ground state. For this, we write the fusion rule

$$e \times e = 1, \tag{11.4.16b}$$

where 1 stands for the ground state or vacuum. Similarly, moving two m-type excitations to the same plaquette creates a closed loop l^{m}, which can be absorbed in the ground state, i.e.,

$$m \times m = 1. \tag{11.4.16c}$$

Superimposing the above processes yields the remaining fusion rules

$$m \times f = e, \qquad e \times f = m, \qquad f \times f = 1. \tag{11.4.16d}$$

It is now imperative to ask what type of quantum statistics these emergent excitations obey. We recall that quantum statistics are defined as the phase by which a state changes if two identical particles are exchanged. Rendering the exchange operation as an adiabatically slow evolution of the state, in three and higher dimensions only two types of statistics are allowed between point particles: that of bosons with phase $+1$ and that of fermions with phase -1. In 2D, richer possibilities exist and the exchange phase ϑ can be *any* complex number on the unit circle, opening the way for *any*ons. While the exchange is only defined for quantum particles of the same type, the double exchange (braiding) is well defined between any two deconfined anyons. We can compute the braiding phases of the anyons e, m, and f that appear in the toric code one by one. Let us start with the phase resulting from braiding e_1 with e_2. The initial state is $W^{\mathrm{e}}_{l^{\mathrm{e}}}|\mathrm{GS}\rangle$ depicted in Fig. 11.5 a). Moving e_1 around e_2 leaves a loop of flipped σ^x bonds around e_2 [see Fig. 11.5 c)]. This loop is created by applying B_p to all plaquettes enclosed by the loop $l^{\mathrm{e}}_{e_1}$ along which e_1 moves. We can thus write the final state as

$$\begin{aligned}\left(\prod_{p\in l^{\mathrm{e}}_{e_1}} B_p\right) W^{\mathrm{e}}_{l^{\mathrm{e}}}|\mathrm{GS}\rangle &= W^{\mathrm{e}}_{l^{\mathrm{e}}}\left(\prod_{p\in l^{\mathrm{e}}_{e_1}} B_p\right)|\mathrm{GS}\rangle \\ &= W^{\mathrm{e}}_{l^{\mathrm{e}}}|\mathrm{GS}\rangle.\end{aligned} \tag{11.4.17}$$

Flipping the spins in a closed loop does not alter the ground state as it is the equal amplitude of all loop configurations. We conclude that the braiding of two e particles gives no phase. Similar considerations can be used to conclude that the braiding of two m particles is trivial as well.

In fact, not only the braiding, but also the exchange of two e particles and two m particles is trivial. (We have not shown that here.)
More interesting is the braiding of m with e. Let the initial state be $W^{\mathrm{m}}_{l^{\mathrm{m}}} W^{\mathrm{e}}_{l^{\mathrm{e}}} |\mathrm{GS}\rangle$ and move the e particle located on one end of the string $l^{\mathrm{e}}_{\mathrm{in}}$ around the magnetic particle m on one end of the string l^{m}. Again this is equivalent to applying B_p to all plaquettes enclosed by the path l^{e}_e of the e particle, so that the final state is given by

$$\begin{aligned}\left(\prod_{p\in l^{\mathrm{e}}_e} B_p\right) W^{\mathrm{m}}_{l^{\mathrm{m}}} W^{\mathrm{e}}_{l^{\mathrm{e}}} |\mathrm{GS}\rangle &= -\, W^{\mathrm{m}}_{l^{\mathrm{m}}} \left(\prod_{p\in l^{\mathrm{e}}_e} B_p\right) W^{\mathrm{e}}_{l^{\mathrm{e}}} |\mathrm{GS}\rangle \\ &= -\, W^{\mathrm{m}}_{l^{\mathrm{m}}} W^{\mathrm{e}}_{l^{\mathrm{e}}} |\mathrm{GS}\rangle .\end{aligned} \tag{11.4.18}$$

The product over B_p operators anticommutes with the path operator $W^{\mathrm{m}}_{l^{\mathrm{m}}}$, because there is a single bond on which a single σ^x and a single σ^z act at the crossing of l^{m} and l^{e}_e [see Fig. 11.5 d)].
As a result, the initial and final state differ by a -1, which is the braiding phase of e with m. Particles with this braiding phase are called (mutual) semions.
Notice that we have moved the particles on contractible loops only. If we create a pair of e or m particles, move one of them along a noncontractible loop on the torus, and annihilate the pair, we have effectively applied the operators $W^{\mathrm{e}}_{x/y}$ and $W^{\mathrm{m}}_{x/y}$ to the ground state (although in the process we have created finite energy states). The operation of moving anyons on noncontractible loops thus allows to operate on the manifold of topologically degenerate groundstates. This exposes the intimate connection between the presence of fractionalized excitations and topological groundstate degeneracy in topologically ordered systems.
From the braiding relations of e and m we can also conclude the braiding and exchange relations of the composite particle f. This is most easily done in a pictorial way by representing the particle worldlines as moving upwards. For example, we represent the braiding relations of e and m as

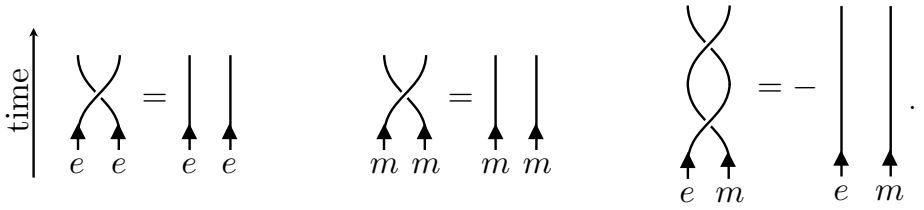

(11.4.19)

The exchange of two f, each of which is composed of one e and one m is then

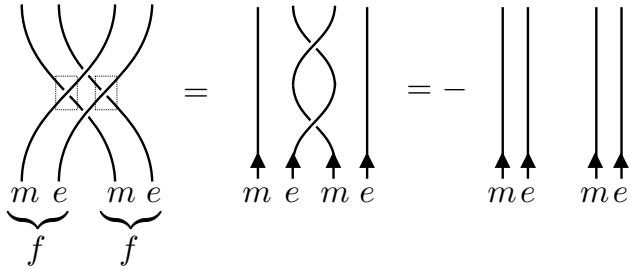

(11.4.20)

Notice that we have used Eq. (11.4.19) to manipulate the crossing in the dotted rectangles. Exchange of two f thus gives a phase -1 and we conclude that f is a fermion.
In summary, we have used the toric code model to illustrate topological ground state degeneracy and emergent anyonic quasiparticles as hallmarks of topological order. We note that the toric code model does not support topologically protected edge states.

References

1. Kitaev, A. Y. & Preskill, J. "Topological Entanglement Entropy". *Phys. Rev. Lett.* **96,** 110404. http://dx.doi.org/10.1103/PhysRevLett.96.110404 (2006).